

Assessment of Experimental Data and Thermodynamic Modeling in the Zr-Fe-O System



OLGA FABRICHNAYA and DMYTRO PAVLYUCHKOV

The thermodynamic parameters of the $\text{ZrO}_2\text{-FeO-Fe}_2\text{O}_3$ system were assessed based on experimental data for the ZrO-FeO and $\text{ZrO}_2\text{-Fe}_3\text{O}_4$ systems for the first time. The solubility of FeO and Fe_2O_3 in the ZrO_2 -based solid solutions and the solubility of ZrO_2 in the Fe_2O_3 and Fe_3O_4 phases were taken into account and described by compound energy formalism. A partially ionic liquid model was used to describe the liquid phase. The isothermal section and liquidus surface of the $\text{ZrO}_2\text{-FeO-Fe}_2\text{O}_3$ system were calculated. Data on binary systems were combined with the description of the $\text{ZrO}_2\text{-FeO-Fe}_2\text{O}_3$ system. Phase diagrams were calculated using a thermodynamic description based on advanced models. An equilibrium between the metallic liquid and solid ZrO_2 was calculated and compared with experimental data. Substantial differences between the calculations and the results of experiments were found, as in the calculations of previous research.

DOI: 10.1007/s11661-015-2805-8

© The Minerals, Metals & Materials Society and ASM International 2015

I. INTRODUCTION

THE interaction of iron with a ZrO_2 ceramic presents an issue of practical interest. The system Zr-O-Fe must be understood to aid in preventing refractories from reacting with metallurgical slag.^[1] The system under investigation was part of a corium system (U-Zr-Fe-O). Thermodynamic modeling of the Zr-Fe-O system is essential for understanding the possible reactions of a melt in the active zone of a nuclear reactor, including the housing materials and reactions occurring during a severe nuclear accident.^[1] The system is also of interest for deoxidation and inclusion shape control in steel.^[2] ZrO_2 that was partially stabilized by 10 mass pct MgO was proposed as a reinforcement component of the TRIP-matrix composite.^[3] Therefore, the Zr-Fe-O system is a key subsystem for simulation of interfacial reactions between steels and ceramic materials.

Experimental data for the Zr-Fe-O system are quite scarce due to difficulties in conducting such experiments.^[3] It should be stressed that the phase equilibria in this system depends on oxygen partial pressures and therefore control of oxygen partial pressures in the experiments is very important. Substantial experimental difficulty is the reaction of samples with crucible material.^[3] However, phase diagrams are available for the $\text{ZrO}_2\text{-FeO}$ system.^[1,4,5] The difference between^[4] and^[1,5] is mainly in the composition of the eutectic reaction $L = \text{FeO (wustite)} + \text{tetragonal-ZrO}_2$. The solubility of FeO in a ZrO_2 fluorite phase was found to be 12, and 2.2 mol pct in the tetragonal phase.^[1,5] The phase diagram of the $\text{ZrO}_2\text{-Fe}_3\text{O}_4$ system in an air

atmosphere was investigated by different authors.^[6,7] The low solubility of ZrO_2 in the Fe_3O_4 magnetite phase (spinel structure) and Fe_2O_3 hematite phase (corundum structure) was found. On the other hand, the ZrO_2 -based phases with tetragonal and cubic fluorite structures were found to dissolve only a small portion of the Fe_3O_4 . Phase relations in the $\text{ZrO}_2\text{-Fe}_3\text{O}_4$ system were investigated by^[8] at an oxygen partial pressure of 2.1×10^{-3} bar.

The isothermal section of a $\text{ZrO}_2\text{-FeO-Fe}_2\text{O}_3$ system at 1473 K (1200 °C) is presented in (Reference 9) based on experimental data at a measured oxygen partial pressure.

Determination of the liquidus temperature in the $\text{ZrO}_2\text{-FeO-Fe}_2\text{O}_3$ system was based on a combination of experiments in an air atmosphere and calculations, and is presented by (Reference 10). Immiscibility in the liquid phase was indicated in the range of 34 to 82 mass pct of ZrO_2 based on the results of X-ray diffraction (XRD) and scanning electron microscopy combined with wavelength-dispersive X-ray spectroscopy (SEM/WDS) investigation of quenched samples.

Fruehan^[11] investigated the equilibrium of a metallic liquid with a tetragonal phase of ZrO_2 at 1953 K (1680 °C). The dependence of the oxygen concentration on the Zr concentration in the metallic liquid was determined for the range of Zr concentration between 0.005 and 1 mass pct. The minimum solubility of oxygen (6 ppt) was found at 0.074 mass pct Zr. Deoxidation equilibria in an Fe-O-Zr system at 1873 K (1600 °C) are investigated by EMF.^[12] The concentration and activity of oxygen in Fe-Zr liquid alloys is determined.

A thermodynamic database of the Zr-Fe-O system was constructed by Huang^[13] based on binary descriptions, and phase diagrams of the ternary system are calculated. However, the oxide part of the system was not fitted to reproduce experimental data from literature. The

OLGA FABRICHNAYA, Principal Researcher, and DMYTRO PAVLYUCHKOV, Postdoctoral Researcher, are with the Institute of Materials Science, TU Bergakademie Freiberg, Gustav-Zeuner-Str. 5, 09599 Freiberg, Germany. Contact e-mail: fabrich@ww.tu-freiberg.de
Manuscript submitted August 5, 2014.

Article published online February 18, 2015

equilibrium between liquid iron and the ZrO_2 tetragonal phase is calculated. The calculated solubility of oxygen vs Zr solubility in the metallic liquid is found to be substantially lower in comparison with experimental data.^[11]

The aim of the present study is to develop a database for the Zr-Fe-O system based on experimental data available in the literature. Novelty of this study is in focus on the oxide part of the system which was not modeled so far. This database will be one of the most important parts of the ceramic and steel databases for modeling relations between steel and ZrO_2 -based ceramics used for the development of TRIP-steel composite materials.

II. THERMODYNAMIC MODELING

The sub-lattice model was applied to describe solution phases, and a partially ionic liquid model was used for description of the liquid. The crystallographic information and thermodynamic models used for phase descrip-

tions are presented in Table I. Thermodynamic description of the Fe-Zr system was accepted from,^[14] for Fe-O from,^[15] and for Zr-O from the unpublished description of Wang.^[16] The Gibbs energies for the ZrO_2 polymorphic modifications could be found in.^[17] Phase diagrams of the Zr-O and Fe-Zr systems are presented in Figures 1(a) and (b).

At the first step of optimization, only the oxides ZrO_2 , FeO, and Fe_2O_3 were considered. Pure Fe phases were included because wustite is an Fe-deficient phase and, therefore, the FeO stoichiometric composition corresponds to the equilibrium of wustite and iron. Data from the literature^[1,4,5] were used to optimize mixing parameters corresponding to interactions between Fe^{+2} and Zr^{+4} species in the liquid phase of ZrO_2 -based solutions. Positive additions to the Gibbs energy parameters of FeO and Fe_2O_3 with ZrO_2 structures (cubic, tetragonal and monoclinic) were selected, with parameters similar to the corresponding structures of MgO and Al_2O_3 . The interaction parameters between Fe^{+3} and Zr^{+4} were then assessed in the ZrO_2 -based phases and the interaction parameter ${}^0L(Zr^{+4}:O^{-2},FeO_{3/2})$. Simultaneously, the low

Table I. Thermodynamic Models Used for Phase Descriptions in the Zr-Fe-O System

Phase Name	Space Group	Model
bcc	<i>Im-3m</i>	$(Fe,Zr)_1(Va,O)_3$
fcc	<i>Fm-3m</i>	$(Fe,Zr)_1(Va,O)_1$
hcp	<i>P6_3/mmc</i>	$(Zr,Fe)_1(Va,O)_{0.5}$
$Fe_{147}Zr_{53}$	<i>P6_3/mmc</i>	$(Fe)_{147}(Zr)_{53}$
C15	<i>Fd-3m</i>	$(Zr,Fe)_2(Zr,Fe)_1$
$FeZr_2$	<i>I4/mcm</i>	$(Zr,Fe)_1(Zr,Fe)_2$
$FeZr_3$	<i>Cmcm</i>	$(Zr,Fe)_1(Zr,Fe)_3$
ZrO_2 fluorite (F)	<i>Fm-3m</i>	$(Zr^{+4},Fe^{+2},Fe^{+3})_1(O^{-2},Va)_2$
ZrO_2 tetragonal (T)	<i>P42/nmc</i>	$(Zr^{+4},Fe^{+2},Fe^{+3})_1(O^{-2},Va)_2$
ZrO_2 monoclinic (M)	<i>P121/c1</i>	$(Zr^{+4},Fe^{+2},Fe^{+3})_1(O^{-2},Va)_2$
Fe_xO wustite (Wu)	<i>Fm-3m</i>	$(Fe^{+2},Fe^{+3},Va)_1(O^{-2})_1$
Fe_3O_4 magnetite (Magn)	<i>Fd-3mZ</i>	$(Fe^{+2},Fe^{+3},Zr^{+4})_1(Fe^{+2},Fe^{+3},Va)_2(Va,Fe^{+2})_2(O^{-2})_4$
Fe_2O_3 hematite (Hem)	<i>R-3cH</i>	$(Fe^{+3},Zr^{+4})_2(Va,O^{-2})_1(O^{-2})_3$
Liquid (L)	—	$(Fe^{+2},Zr^{+4})_p(O^{-2},FeO_{1.5},Va)_Q$

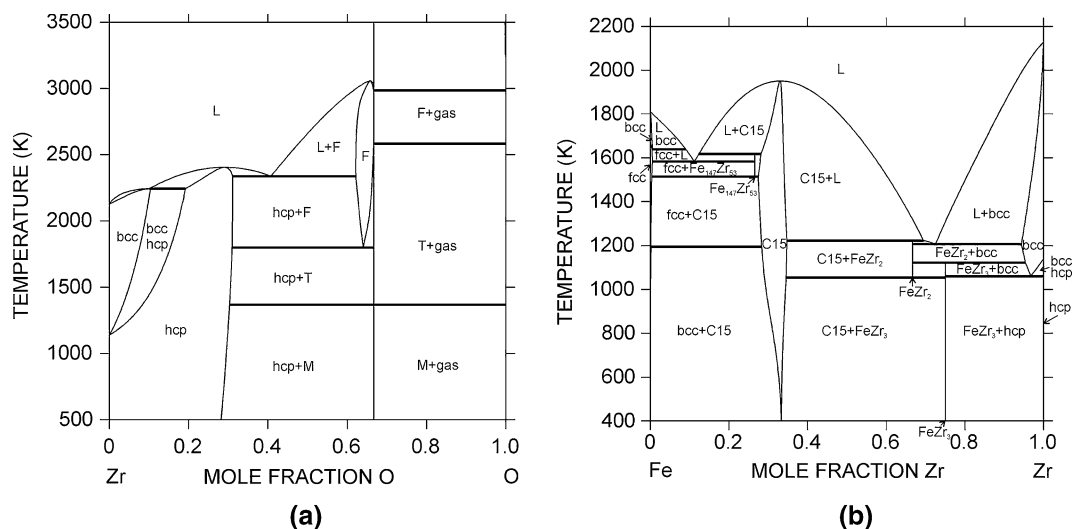
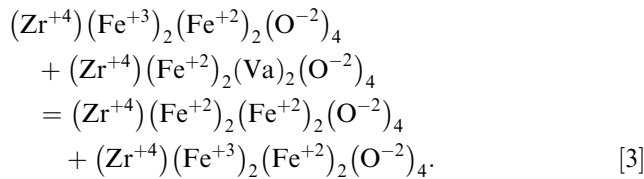
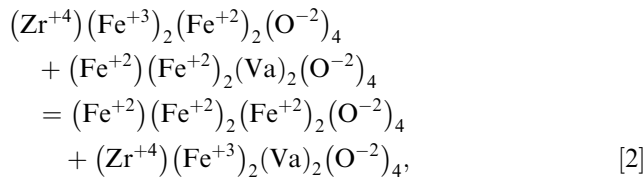
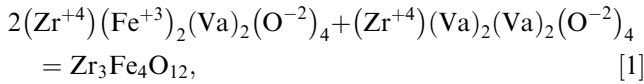


Fig. 1—*a, b*—Calculated phase diagrams for binary systems. *a* Zr-O; *b* Fe-Zr.

solubility of ZrO_2 in the Fe_2O_3 (hematite) corundum structure was taken into account, and corresponding G parameters of the ZrO_2 end members with corundum structures were assessed. To assess these parameters, experimental data from^[6,7] were included in the optimization. In the next step of optimization, the solubility of ZrO_2 in an Fe_3O_4 (magnetite) spinel structure was taken into account. As suggested by,^[7] Zr^{+4} can occupy tetrahedral sites in the spinel structure. Therefore, the following model was applied to spinel (Fe^{+3} , Fe^{+2} , Zr^{+4})₁(Fe^{+2} , Fe^{+3} , Va)₂(Va, Fe^{+2})₂(O^{-2})₄, where Va stands for vacancy. The Gibbs energies of fictive end-members were determined using reactions for electro-neutrality conditions (1) and reciprocal reactions (2,3):



The Gibbs energies for the two neutral compounds (Zr^{+4})₁(Fe^{+2})₂(Va)₂(O^{-2})₄ and (Zr^{+4})₁(Va)₂(Fe^{+2})₂(O^{-2})₄ were described as the sum of the Gibbs energies of the oxides ZrO_2 and FeO plus the optimized parameters a_1 and $b_1 \cdot T$, which were different for these two compounds (see Table II):

$$G(ZrFe_2O_4) = G(ZrO_2) + 2G(FeO) + a_1 + b_1 \cdot T. \quad [4]$$

The Gibbs energy of the $Zr(Va)_2(Va)_2O_4$ compound was described as the sum of the Gibbs energy of ZrO_2 and O_2 . The Gibbs energy of the $Zr_3Fe_4O_{12}$ neutral compound was described as the sum of the oxides ZrO_2 and Fe_2O_3 plus the optimized parameters a_2 and $b_2 \cdot T$:

$$G(Zr_3Fe_4O_{12}) = 2G(ZrFe_2O_4) + G(ZrVaVaO_4) + a_2 + b_2 \cdot T + 6RT(2/3 \ln(2/3) + 1/3 \ln(1/3)), \quad [5]$$

where the last term is a configuration entropy contribution.

The Gibbs energies for $Zr(Fe^{+3})_2(Fe^{+2})_2(O^{-2})_4$ and $Zr(Fe^{+2})_2(Fe^{+2})_2(O^{-2})_4$ were derived from a reciprocal reaction including optimized parameters. In order to model the solubility of ZrO_2 , the Gibbs energies of the included magnetite's end members were optimized using the experimental data of.^[6-8] The thermodynamic

parameters optimized in the present work are listed in Table II. At the final stage of the Zr-Fe-O system database development, the parameters of metallic phases and the corresponding Gibbs energies of the liquid metal (Lm) as well as the interaction parameters in the ionic liquid phase were introduced from the descriptions of the binary systems.

III. RESULTS AND DISCUSSION

The calculated phase diagram of the ZrO_2 - FeO system together with experimental data is presented in Figure 2(a). The calculated liquidus curve is in good agreement with the experimental data of.^[1,4] The eutectic composition was equal to 7 mol pct of ZrO_2 by calculation. This value is in between the values obtained by Bechta *et al.*^[1] (12 mol pct) and Fisher and Hoffmann^[4] (3 mol pct). It should be mentioned that extension of the system through the inclusion of metallic phases and a metal part description into the ionic liquid phase does not lead to substantial changes in the invariant reaction data (see Figure 2(b)). However, the presence of two liquids (metallic Lm and oxide Lox) was calculated in equilibrium with fluorite and tetragonal phases as well as a liquid miscibility gap.

The calculated phase diagrams of the ZrO_2 - Fe_3O_4 system at an oxygen partial pressure of 0.21 bar and 2.1×10^{-3} bar are presented in Figures 3(a) and (b) along with the available experimental data.^[6,7] The calculated temperatures of the reactions $T + \text{Magn} = \text{Hem}$ at 1670 K (1397 °C) and $L = \text{Magn} + T$ at 1801 K (1528 °C) at air conditions are in good agreement with the experimental data of (Reference 6) at 1707 K and 1798 K (1434 °C and 1525 °C), respectively, though the eutectic composition (80.4 mol pct Fe_3O_4) was quite different from value of 69.4 mol pct presented in the phase diagram of (Reference 6). However, there is very scarce information about this diagram and the method by which the composition of the eutectic was determined. Also the method which was used to determine magnetite and hematite compositions as well as their uncertainty were not mentioned in (Reference 6). Therefore, new experimental data on eutectic composition and maximal solubility determination of ZrO_2 in magnetite and hematite are desirable. The calculated maximal solubility of ZrO_2 in magnetite is 1 and 2.9 mol pct in hematite. The calculated maximal solubility of Fe_2O_3 in tetragonal modification of ZrO_2 is 2.5 mol pct. These values are in reasonable agreement with those of,^[7] with 6 mol pct of ZrO_2 in hematite and 3 mol pct of Fe_2O_3 in the ZrO_2 phase. Furthermore, the temperature of the invariant reaction $\text{Magn} + T = \text{Hem}$, determined as 1710 K (1437 °C) by^[7] is consistent with previous work.^[6] It was reproduced reasonably well in the calculations of this work.

The comparison of calculations (Figure 3(b)) with experimental data shows substantial differences in the temperature of the invariant reaction $T + \text{Magn} = \text{Hem}$ between the calculated value of 1483 K (1210 °C) and the experimental one of^[8] at 1573 K (1300 °C) at 2.1×10^{-3} oxygen partial pressure. The reason for such difference

Table II. Assessed Thermodynamic Parameters

Phase	Assessed Thermodynamic Parameters (J/mol)
Liquid (L)	${}^0L_{\text{Fe}^{+2},\text{Zr}^{+4},\text{O}^{-2}}^{\text{Liquid}} = -17320.87$
	${}^1L_{\text{Fe}^{+2},\text{Zr}^{+4},\text{O}^{-2}}^{\text{Liquid}} = -3683$
	${}^0L_{\text{Zr}^{+4},\text{O}^{-2},\text{FeO}_{2/3}}^{\text{Liquid}} = 41044.94$
	${}^1L_{\text{Zr}^{+4},\text{O}^{-2},\text{FeO}_{2/3}}^{\text{Liquid}} = -17769.3$
ZrO ₂ Fluorite (F)	${}^0G_{\text{Fe}^{+2},\text{O}^{-2}}^{\text{ZrO}_2\text{-cub}} = \text{GWUSTITE} + \text{GHSEROO} + 45000 + 11.5263T$
	${}^0G_{\text{Fe}^{+3},\text{O}^{-2}}^{\text{ZrO}_2\text{-cub}} = 0.5\text{GZRO2C} + 0.5\text{GHSEROO} + 50000 + 9.35T$
	${}^0G_{\text{Fe}^{+2},\text{Va}}^{\text{ZrO}_2\text{-cub}} = \text{GWUSTITE} - \text{GHSEROO} + 45000 + 11.5263T$
	${}^0G_{\text{Fe}^{+3},\text{Va}}^{\text{ZrO}_2\text{-cub}} = 0.5\text{GFE2O3} - 1.5\text{GHSEROO} + 50000 + 9.35T$
	${}^0L_{\text{Fe}^{+2},\text{Zr}^{+4},\text{O}^{-2}}^{\text{ZrO}_2\text{-cub}}(\text{Va}) = 15000$
	${}^0L_{\text{Fe}^{+3},\text{Zr}^{+4},\text{O}^{-2}}^{\text{ZrO}_2\text{-cub}}(\text{Va}) = 9250$
ZrO ₂ Tetragonal(T)	${}^0G_{\text{Fe}^{+2},\text{O}^{-2}}^{\text{ZrO}_2\text{-tet}} = \text{GWUSTITE} + \text{GHSEROO} + 60000 + 11.5263T$
	${}^0G_{\text{Fe}^{+3},\text{O}^{-2}}^{\text{ZrO}_2\text{-tet}} = 0.5\text{GZRO2C} + 0.5\text{GHSEROO} + 50000 + 9.35T$
	${}^0G_{\text{Fe}^{+2},\text{Va}}^{\text{ZrO}_2\text{-tet}} = \text{GWUSTITE} - \text{GHSEROO} + 60000 + 11.5263T$
	${}^0G_{\text{Fe}^{+3},\text{Va}}^{\text{ZrO}_2\text{-tet}} = 0.5\text{GFE2O3} - 1.5\text{GHSEROO} + 50000 + 9.35T$
	${}^0L_{\text{Fe}^{+2},\text{Zr}^{+4},\text{O}^{-2}}^{\text{ZrO}_2\text{-tet}}(\text{Va}) = 50000$
	${}^0L_{\text{Fe}^{+3},\text{Zr}^{+4},\text{O}^{-2}}^{\text{ZrO}_2\text{-tet}}(\text{Va}) = 10000$
ZrO ₂ Monoclinic(M)	${}^0G_{\text{Fe}^{+2},\text{O}^{-2}}^{\text{ZrO}_2\text{-mon}} = \text{GWUSTITE} + \text{GHSEROO} + 120000 + 11.5263T$
	${}^0G_{\text{Fe}^{+3},\text{O}^{-2}}^{\text{ZrO}_2\text{-mon}} = 0.5\text{GZRO2C} + 0.5\text{GHSEROO} + 100000 + 9.35T$
	${}^0G_{\text{Fe}^{+2},\text{Va}}^{\text{ZrO}_2\text{-mon}} = \text{GWUSTITE} - \text{GHSEROO} + 120000 + 11.5263T$
	${}^0G_{\text{Fe}^{+3},\text{Va}}^{\text{ZrO}_2\text{-mon}} = 0.5\text{GFE2O3} - 1.5\text{GHSEROO} + 100000 + 9.35T$
Fe ₂ O ₃ Hematite (Hem)	${}^0G_{\text{Zr}^{+4},\text{O}^{-2},\text{O}^{-2}}^{\text{Hematite}} = 2\text{GZRO2C} + 50000$
	${}^0G_{\text{Zr}^{+4},\text{Va},\text{O}^{-2}}^{\text{Hematite}} = 2\text{GZRO2C} - \text{GHSEROO} + 50000$
	${}^0L_{\text{Fe}^{+3},\text{Zr}^{+4},\text{O}^{-2}}^{\text{Hematite}}(\text{Va})\text{O}^{-2} = 120000$
Fe ₃ O ₄ Magnetite (Magn)	${}^0G_{\text{Zr}^{+4},\text{Fe}^{+3},\text{Fe}^{+2},\text{O}^{-2}}^{\text{Magnetite}} = 2\text{GFE3O4} + \text{DFE3O4} - \text{BFE3O4} + \text{GZRO2C} + 4\text{GWUSTITE} + \text{GHSEROO} - \text{GFE2O3} + 140000 - 15.8767T$
	${}^0G_{\text{Zr}^{+4},\text{Fe}^{+3},\text{Fe}^{+2},\text{O}^{-2}}^{\text{Magnetite}} = 2\text{GFE3O4} + \text{DFE3O4} - \text{BFE3O4} + \text{GZRO2C} + 2\text{WUSTITE} + 70000$
	${}^0G_{\text{Zr}^{+4},\text{Va},\text{Fe}^{+2},\text{O}^{-2}}^{\text{Magnetite}} = \text{GZRO2C} + 2\text{WUSTITE} + 70000$
	${}^0G_{\text{Zr}^{+4},\text{Fe}^{+2},\text{Va},\text{O}^{-2}}^{\text{Magnetite}} = \text{GZRO2C} + 2\text{WUSTITE} + 60000$
	${}^0G_{\text{Zr}^{+4},\text{Fe}^{+3},\text{Va},\text{O}^{-2}}^{\text{Magnetite}} = \text{GZRO2C} - \text{GHSEROO} + \text{GFE2O3} + 60000 + 15.8767T$
	${}^0G_{\text{Zr}^{+4},\text{Va},\text{Va},\text{O}^{-2}}^{\text{Magnetite}} = \text{GZRO2C} + 2\text{GHSEROO}$

Functions GZRO2L, GZRO2C, GZRO2T, GZRO2M are taken from Wang *et al.*,^[17] GHSEROO, GWUSTITE, GFE2O3, GFE3O4, DFE3O4, BFE3O4 are taken from Kjellquist *et al.*^[15].

can be the uncertainty of oxygen partial pressure control, since at air condition the agreement between calculations and experimental data of the same authors was better.^[7]

The substantial difference between the calculations and the accepted data in^[8] for magnetite-hematite transformation in a binary Fe-O system should be mentioned. The

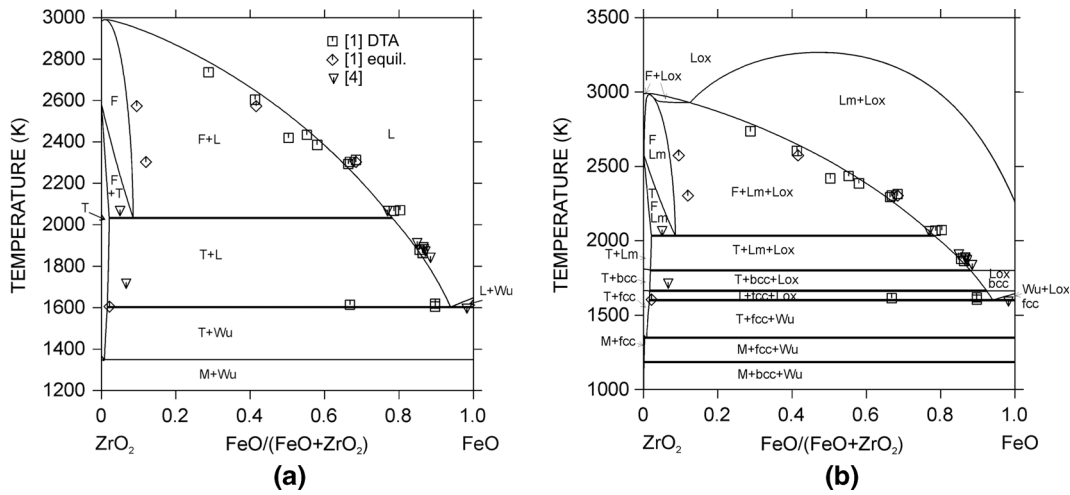


Fig. 2—*a, b*—Phase diagram of the ZrO₂-FeO system calculated using. *a* Simplified dataset including oxides and pure Fe. *b* Advanced dataset of the Zr-Fe-O system.

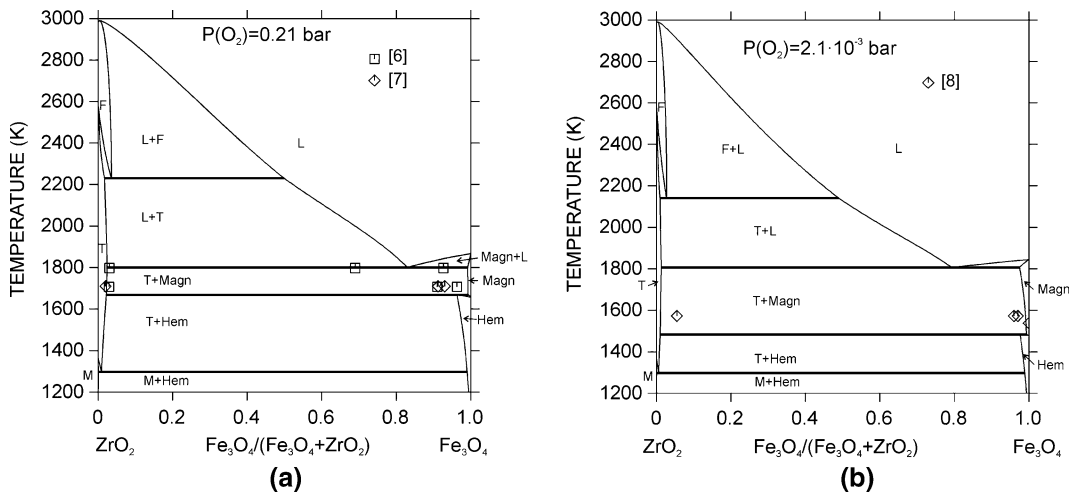


Fig. 3—*a, b*—Calculated phase diagram of the ZrO₂-Fe₃O₄ system. *a* At air conditions $P(O_2) = 0.21$; *b* at $P(O_2) = 2.1 \times 10^{-3}$ bar.

calculated temperature of magnetite to hematite transformation is 1478 K (1205 °C) which is lower than 1538 K (1265 °C) measured in the work.^[8] The calculation is based on thermodynamic description of Kjellqvist *et al.*^[15] where all available data in the Fe-O system were critically assessed and optimized. This difference in binary system Fe-O between calculation and experimental data^[8] at $P(O_2) = 2.1 \times 10^{-3}$ bar indicated the same trend as in the ZrO₂-Fe₃O₄ system.

The calculated isothermal section of the ZrO₂-FeO-Fe₂O₃ system at 1473 K (1200 °C) is presented in Figure 4. The calculated partial pressure of oxygen is shown in the three-phase fields as $\lg P(O_2)$, where $P(O_2)$ is expressed in bar. Katsura *et al.*^[9] measured the oxygen partial pressures by solid electrolyte cell for equilibrated mixtures Fe₂O₃ and ZrO₂ inside the furnace with temperature control ± 1 °C. The studied mixtures represented two-phase equilibria Wu + T and Magn + T. According to their results $\lg P(O_2)$ changed from -11.82 to -9.21 in Wu + T phase field and

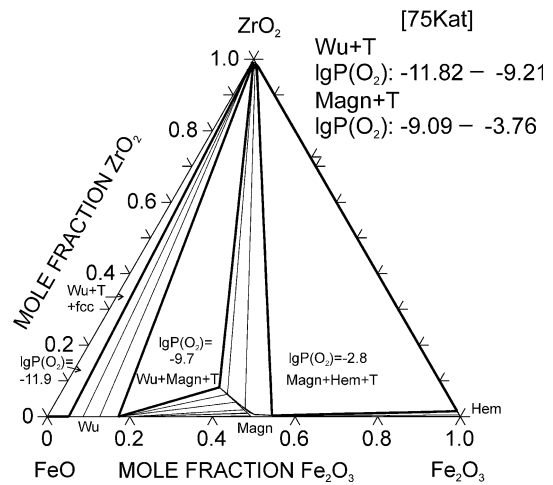


Fig. 4—Isothermal section of the ZrO₂-FeO-Fe₂O₃ system calculated at 1473 K (1200 °C).

from -9.09 to -3.76 in Magn + T phase field. At higher $\lg P(\text{O}_2)$, where hematite phase formed, the measurements were not done in work.^[9] It should be mentioned that the calculated partial pressures for the Fe + Wu + T and Magn + Hem + T phase assemblages ($\lg P(\text{O}_2) = -11.9$ and $\lg P(\text{O}_2) = -2.8$, respectively) are consistent with the ranges measured by,^[9] while for Wu + Magn + T , the calculated partial pressure of oxygen is lower ($\lg P(\text{O}_2) = -9.7$) than the value from^[9] (it should be between -9.21 and -9.09). The consistent value (-9.19) that was calculated for this field in the case of the ZrO_2 solubility in magnetite was not taken into account. Solubility of ZrO_2 in magnetite therefore leads to decrease of oxygen partial pressure. The calculated solubility of ZrO_2 in magnetite (8 mol pct) was higher than that measured by^[9] (3 mol pct). The method used by^[9] to determine composition of the phases was not mentioned.

The calculated liquidus surface is presented in Figure 5. The calculated liquidus temperatures of invariant reactions and the composition of the liquid are presented in Table III. Liquidus projection was also carried out in the work of Petrov *et al.*^[10] based on experimental data and calculations. The models and thermodynamic data used in these calculations were not presented in the work.^[10] The authors found several indications of phase separation in the liquid phase at compositions of 34 to 82 mass pct of ZrO_2 in the $\text{ZrO}_2\text{-FeO}_x$ system in an air atmosphere and at a temperature range of between

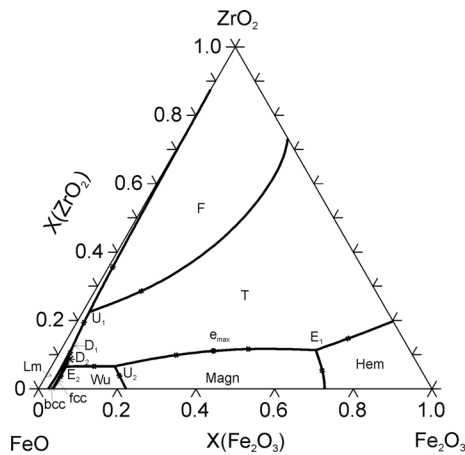


Fig. 5—Liquidus surface of the $\text{ZrO}_2\text{-FeO-Fe}_2\text{O}_3$ system calculated using advanced thermodynamic description of the Zr-Fe-O system.

2143 K and 2503 K (1870 °C and 2230 °C). The solubility of 6.6 mass pct of FeO_x in $\text{ZrO}_2\text{-M}$ seems to be too high, while the solubility of ZrO_2 in magnetite equal to 2.5 mass pct is consistent with other data.^[6,7] Non-equilibrium crystallization and high levels of impurities should be mentioned, as well as observation of the hexagonal structure of ZrO_2 , which is unknown in the literature. Therefore, the results obtained in^[10] are dubious and the liquidus diagram needs to be re-investigated. Comparison of the results of calculations for invariant reactions performed in the present study and calculations of^[10] indicates substantial differences in temperature and liquid composition. Furthermore, calculations performed in the present study do not exhibit any miscibility gap. New experimental study of melting relations is necessary to resolve this contradiction.

The calculated solubility of oxygen in the metallic liquid phase against the concentration of Zr for an equilibrium between the metallic liquid and the $\text{ZrO}_2\text{-T}$ is shown in Figure 6(a) for the two temperatures 1873 K and 1953 K (1600 °C and 1680 °C) along with the experimental data of^[11] and^[12] There is substantial inconsistency between the calculated and experimental data. It should be mentioned that the same inconsistency was observed in the calculations of.^[12,13] It is shown in the work of^[13] and in the present work that introduction of the negative ternary interaction parameter does not improve the fit. In the work of,^[13] the better fit was obtained by changing the enthalpy of tetragonal ZrO_2 phase substantially. Obviously, this could not be used as a solution to the problem because such change would also dramatically alter the Zr-O phase diagram. The calculations of^[18] show better consistency with the results of^[11,12] in the range 0.1 to 3 mass pct Zr. At lower Zr contents, the calculated oxygen solubility is one order of magnitude lower than the experimental values. Huang^[13] compared calculations for similar systems of type Fe-M-O (where M denotes a strong deoxidizer of Fe), and concluded that experimental solubility measurements may include systematic errors. This assumption is based on the fact that according to,^[11] the oxygen solubility in Fe-Zr-O, Fe-Ce-O, Fe-La-O and Fe-Al-O systems are about the same. However, this is not likely because the stabilities of oxides are different. The same conclusion about high experimental error was made by Hillert and Selleby^[19] based on comparison of calculations with available experimental data for the systems Fe-Ca-O and Fe-Al-

Table III. Calculated Data for Invariant Reactions in the $\text{ZrO}_2\text{-FeO-Fe}_2\text{O}_3$ System

Reaction	Type	Temperature [K (°C)]	Liquid Composition (Mol Pct)		
			ZrO ₂	FeO	Fe ₂ O ₃
$L + F = \text{Fe}(\text{liq}) + T$	U ₁	2032 (1759)	22.46	75.86	1.68
$L = T + \text{Magn}$	e _{max1}	1815 (1442)	11.52	43.95	44.53
$L = T + (\text{bcc} + \text{Lm})$	D ₁	1803 (1530)	12.65	84.87	2.48
$L = T + \text{Magn} + \text{Hem}$	E ₁	1770 (2034)	11.34	23.83	64.83
$L = T + (\text{bcc} + \text{fcc})$	D ₂	1664 (1937)	8.14	88.59	3.27
$L + \text{Magn} = \text{Wu} + T$	U ₂	1644 (1917)	6.61	77.26	16.13
$L = \text{fcc} + \text{Wu} + T$	E ₂	1602 (1875)	6.46	89.81	3.73

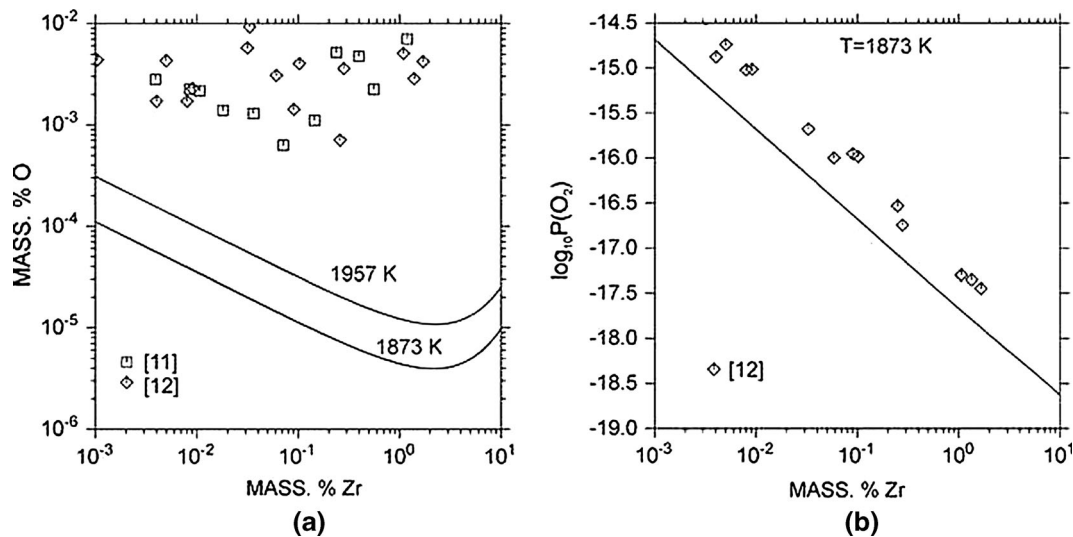


Fig. 6—Calculated equilibrium between metallic liquid and ZrO_2 (T) along with experimental data. *a* Solubility of oxygen (T) vs solubility of Zr in metallic liquid. *b* Oxygen activity in the form of partial pressure of O_2 vs Zr solubility in metallic liquid.

O. Figure 6(b) shows the calculated oxygen partial pressure for the same equilibrium at 1873 K (1600 °C) in comparison with experimental data from.^[12] The consistency between calculations and experiments are better though a shift in $\lg P(O_2)$ equal to ~ 0.5 is observed. Thus the calculated oxygen partial pressures are lower than the experimental data of.^[12]

IV. CONCLUSIONS

A thermodynamic database for the Zr-Fe-O system was developed using CALPHAD approach which allow us to indicate existing contradictions in literature data, to recommend new key experiments for resolving the existing inconsistencies and to reduce amounts of experiments.^[20] Literature data for phase equilibria in the ZrO_2 -FeO, ZrO_2 - Fe_3O_4 , and ZrO_2 -FeO- Fe_2O_3 systems were used for optimization. It should be mentioned that experimental data are scarce and somewhat unreliable. However, the available phase diagrams for the ZrO_2 -FeO system in the presence of Fe and ZrO_2 - Fe_3O_4 systems at air conditions were reproduced by calculation. The solubility of ZrO_2 in Fe_3O_4 magnetite and Fe_2O_3 hematite is taken into account as well as the solubility of FeO and Fe_2O_3 in the ZrO_2 -based solid solutions, and were described by a sub-lattice model by means of compound energy formalism.^[20] The thermodynamic parameters for the ZrO_2 -FeO- Fe_2O_3 system were assessed for the first time using CALPHAD approach. Thermodynamic descriptions of the metallic parts of binary systems were combined with ZrO_2 -FeO- Fe_2O_3 system description into the Zr-Fe-O database. Liquid was described as a single phase using a partially ionic liquid model which allow to describe both metallic and oxide liquids.^[20] The substantial difference between the calculated and experimentally measured solubility of oxygen in the Fe-Zr alloy in equilibrium with ZrO_2 was observed, as it was in other works.^[13,18] Therefore, a preliminary

thermodynamic description of the Zr-Fe-O system was developed. New experimental investigations would be desirable to improve thermodynamic description. The database obtained is a core system for calculating equilibria at the interface between ZrO_2 -based material and TRIP steel in corresponding composite materials.

ACKNOWLEDGMENTS

The authors would like to thank the German Research Foundation (DFG) for its financial support of the Collaborative Research Center Trip-Matrix Composites (SFB799).

REFERENCES

1. S.V. Bechta, E.V. Krushilov, V.I. Almjashev, S.A. Vitol, L.P. Mezentsev, Y.B. Petrov, D.B. Lopuch, V.B. Khabensky, M. Barrachin, S. Hellmann, K. Froment, M. Fischer, W. Tromm, D. Bottomley, F. Defoort, and V.V. Gusarov: *J. Nucl. Mater.*, 2006, vol. 348, pp. 114–21.
2. V. Raghavan: *Phase Diagr. Ternary Iron Alloys*, 1989, vol. 5, pp. 374–79.
3. H. Biermann, U. Martin, A. Aneziris, A. Kolbe, A. Müller, W. Schärfl, and M. Herrman: *Adv. Eng. Mater.*, 2009, vol. 11, pp. 1000–06.
4. W.A. Fischer and A. Hoffmann: *Arch. Eisenhüttenwes*, 1957, vol. 28, pp. 739–43.
5. S.V. Beshta, E.V. Krushilov, V.I. Almjashev, S.A. Vitol, L.P. Mezentsev, Y.B. Petrov, D.B. Lopukh, V.B. Khabenskii, M. Barrachin, S. Hellmann, and V.V. Gusarov: *Rus. J. Inorg. Chem.*, 2006, vol. 51, pp. 325–31.
6. T.S. Jones, S. Kimura, and A. Muan: *J. Am. Ceram. Soc.*, 1967, vol. 50, pp. 137–42.
7. R.H.G.A. Kiminami: *Ceramica (Sao Paulo)*, 1987, vol. 33 (213), pp. 07–09.
8. R.H.G.A. Kiminami: *Ceramica (Sao Paulo)*, 1988, vol. 34 (213), pp. 121–23.
9. T. Katsura, M. Wakihara, S.I. Hara, and T. Sugihara: *J. Solid State Chem.*, 1975, vol. 13, pp. 107–13.

10. Y.B. Petrov, Y.P. Udalov, J. Slovak, and Y.G. Morozov: *Glass Phys. Chem.*, 2002, vol. 28, pp. 139–46.
11. R.J. Fruehan: *Metall. Trans.*, 1974, vol. 5, pp. 345–47.
12. D. Janke and W.A. Fischer: *Arch. Eisenhüttenwes*, 1976, vol. 47, pp. 195–98.
13. W. Huang: *CALPHAD*, 2004, vol. 28, pp. 153–57.
14. P.-Y. Chevalier and E. Fischer: Unpublished Research, 2003, cited by Landolt-Bernstein, *Thermodynamic Properties of Inorganic Materials compiled by SGTE, Group IV (Physical Chemistry), Binary systems—subvolume B, Binary systems from Cs-K to Mg-Zr*, Springer, Berlin, 2005.
15. L. Kjellquist, M. Selleby, and B. Sundman: *CALPHAD*, 2008, vol. 32, pp. 577–92.
16. C. Wang: unpublished research, 2006.
17. C. Wang, M. Zinkevich, and F. Aldinger: *J. Am. Ceram. Soc.*, 2006, vol. 89, pp. 3751–58.
18. I.-H. Jung, S.A. Decterov, and A.D. Pelton: *Metall. Mater. Trans. B*, 2004, vol. 35B, pp. 493–507.
19. M. Hillert and M. Selleby: *Scand. J. Metall.*, 1990, vol. 19, pp. 23–25.
20. H.L. Lukas, S.G. Fries, and B. Sundman: *Computational Thermodynamics. The CALPHAD Method*, Cambridge University Press, Cambridge, 2007.